Resonance Absorption of Gammas by Impurity Nuclei in Crystals*†

WILLIAM M. VISSCHER
Los Alamos Scientific Laboratory, University of California, Los Alamos, New Mexico
(Received 6 August 1962)

The aspects of the dynamics of a simple cubic crystal model with a dilute impurity which are relevant to the Mössbauer effect are considered. Harmonic nearest-neighbor forces are used, and the mass and force constant of the active nucleus differ from those of the host lattice. The calculations are carried out using a Green's function approach with the aid of an IBM 7090 computer. The recoilless fraction, temperature shift, frequencies and amplitudes of localized mode, and absorption spectra are calculated as functions of temperature, impurity mass, and coupling constant. One interesting feature of the results is that the recoilless fraction is independent of the properties of the host lattice over a fairly wide range of variation of mass and force constant. Others are that, in general, the absorption spectrum is not simple related to the phonon spectrum, and that there sometimes exists an approximate low-frequency localized mode.

I. INTRODUCTION

THE magnitude of the Mössbauer effect depends on the recoilless fraction f (Debye-Waller factor). This factor has, since the discovery of the Mössbauer effect, only been calculated in certain limiting cases—the continuum crystal[1] (Debye model) and the high-temperature limit.[2] Although the Debye model has proved to be very useful in practice, it takes no account of the fact that the Mössbauer-active atom is usually an impurity in the crystal. It is one of the aims of the present paper to determine the effect of variation of the impurity parameters on f. We also calculate other observables, such as the velocity shift[3] attributable to lattice dynamics, and the shape of the wings of the Mössbauer spectrum and its relation to the vibration spectrum of the crystal.[4]

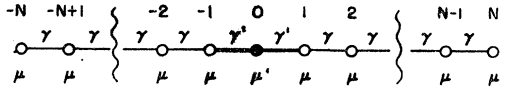

FIG. 1. The linear chain. All the masses and coupling constants are equal except the center mass and its coupling to its neighbors. Periodic boundary conditions are assumed; the $(N+1)$st atom will have the same displacement as the $-N$th.

We use the simple-cubic, harmonic nearest-neighbor force, crystal model which was used by Montroll and Potts,[5] and also much of their notation. In order to keep the numerical work manageable in the final stages we also let the shear and compressional forces be equal. The use of such a restricted model means that we should not expect the results of the calculation to agree very closely with experimental data, but any significant generalization (namely, next nearest neighbor, or anharmonic forces) would greatly complicate the problem. Our impurity is substitutional at a lattice site. When the mismatch between the effective sizes of the host and impurity atoms is great (large atom in a small hole or vice versa) one might expect the effects of anharmonicity to be important.

In Sec. II the one-dimensional case is considered, for which certain of the sums can be performed analytically. Here, the general features of the imperfect lattice spectrum are derived, such as the localized modes of both high[5] and low[6] frequency. Section III contains an exposition of the three-dimensional problem, the determination of the lattice vibrational spectrum, and formulates expressions for the various observables. In Sec. IV the numerical methods are discussed and the results are presented. The final section consists of summary and comparison of the results with the few existing experimental data.

II. A SIMPLE ONE-DIMENSIONAL MODEL

To illustrate the methods we use in the three-dimensional case we now consider a linear chain of atoms (Fig. 1) connected by springs. The center atom has a mass and spring constant different from the rest. The Hamiltonian for this system is

$$H_0=\tfrac{1}{2}\sum_{i=-N}^{N}\mu\dot{x}_i^2+\tfrac{1}{2}\sum_{i=-N}^{N}\gamma(x_i-x_{i-1})^2 +\tfrac{1}{2}\delta\mu\dot{x}_0^2+\tfrac{1}{2}\delta\gamma[(x_1-x_0)^2+(x_{-1}-x_0)^2]. \quad (1)$$

* Work performed under the auspices of the U. S. Atomic Energy Commission.

† A preliminary report of this work was given at the Evanston Meeting of the American Physical Society in June 1962 [Bull. Am. Phys. Soc. **7**, 402 (1962)].

[1] A review of theory and experiment in the Mössbauer effect is contained in H. Frauenfelder, *The Mössbauer Effect* (W. A. Benjamin Inc., New York, 1962). *Note added in proof.* Yu. Kagan and Ya. A. Iosilevskii [J. Exptl. Theoret. Phys. (U.S.S.R.) **42**, 259 (1962) [translation: Soviet Phys.—JETP **15**, 182 (1962)]] have calculated expressions for the Debye-Waller factor for an isolated impurity, which they evaluate in the limit of large impurity mass. These authors use a model for the crystal which is inconsistent with Newton's third law, however, and their results for force constant changes should be used with caution. Dawber and Elliott [P. G. Dawber and R. J. Elliott, Clarendon Laboratory, Oxford (unpublished)] have obtained numerical results which are in substantial agreement with those of the present paper for the case of an isotopic (mass change only) impurity.

[2] A. A. Maradudin and P. A. Flinn, Phys. Rev. **126**, 2059 (1962).

[3] B. D. Josephson, Phys. Rev. Letters **4**, 341 (1960); R. V. Pound and G. A. Rebka, *ibid.* **4**, 274 (1960).

[4] W. M. Visscher, Ann. Phys. (New York) **9**, 194 (1960).

[5] E. W. Montroll and R. B. Potts, Phys. Rev. **100**, 525 (1955); **102**, 72 (1955).

[6] R. Brout and W. Visscher, Phys. Rev. Letters **9**, 54 (1962).

Because the recoilless fraction is of the form[7]

$$f=e^{-2W},$$
$$W=\tfrac{1}{2}\langle(\mathbf{k}\cdot\mathbf{x}_0)^2\rangle_T, \tag{2}$$

where $\mathbf{k}$ is the gamma-ray wave vector, it proves to be convenient to add to the Hamiltonian a term proportional to x_0^2. Then, as shown later, W can be obtained from the total energy by differentiation. Thus, we let

$$H=H_0+H_1,$$
$$H_1=\tfrac{1}{2}a(\mathbf{k}\cdot\mathbf{x}_0)^2. \tag{3}$$

The classical equations of motion, from which we can obtain the normal mode frequencies, are

$$\begin{aligned}\mu\ddot{x}_i-\gamma(x_{i+1}-2x_i+x_{i-1})&=\delta_{i,0}[-\delta\mu\ddot{x}_0+\delta\gamma(x_1-2x_0+x_{-1})+ak^2x_0]\\&\quad+\delta_{i,1}\delta\gamma(x_0-x_1)+\delta_{i,-1}\delta\gamma(x_0-x_{-1}).\end{aligned} \tag{4}$$

We abbreviate them by

$$\sum_\beta L_{\alpha\beta}x_\beta=\sum_\beta P_{\alpha\beta}x_\beta, \tag{5}$$

where

$$\begin{aligned}L_{\alpha\beta}&=\delta_{\alpha\beta}(-\mu\omega^2+2\gamma)-\gamma(\delta_{\alpha+1,\beta}+\delta_{\alpha,\beta+1}),\\P_{\alpha\beta}&=\delta_{\alpha\beta}\delta_{\beta0}(\delta\mu\omega^2-2\delta\gamma-ak^2)+[\delta_{\alpha0}(\delta_{\beta1}+\delta_{\beta-1})\\&\quad+\delta_{\alpha1}(\delta_{\beta0}-\delta_{\beta1})+\delta_{\alpha-1}(\delta_{\beta0}-\delta_{\beta-1})]\delta\gamma.\end{aligned} \tag{6}$$

Now define $g_{\alpha\beta}$ by

$$\textstyle\sum_\beta L_{\alpha\beta}g_{\beta\gamma}=\delta_{\alpha\gamma}, \tag{7}$$

whence, as we show below,

$$g_{\alpha\beta}=\sum_\mu \frac{u_\alpha^{(\mu)}\tilde{u}_\beta^{(\mu)}}{\lambda_\mu} \tag{8}$$

in which the u's are eigenvectors of the linear operator L

$$\textstyle\sum_\beta L_{\alpha\beta}u_\beta^{(\mu)}=\lambda_\mu u_\alpha^{(\mu)}, \tag{9}$$

$$u_\alpha^{(\mu)}=\frac{1}{(2N+1)^{1/2}}e^{i\alpha\varphi_\mu}, \tag{10}$$

$$\lambda_\mu=4\gamma\sin^2(\tfrac{1}{2}\varphi_\mu)-\mu\omega^2. \tag{11}$$

In Eq. (10) the φ's are chosen such that the u's satisfy periodic boundary conditions

$$e^{-iN\varphi_\mu}=e^{i(N+1)\varphi_\mu},$$
$$(2N+1)\varphi_\mu=2n\pi,\quad n=-N,\ -N+1,\ \cdots+N. \tag{12}$$

[7] The recoilless fraction is actually $\exp(-2W)$ times a correction factor involving Bessel functions of imaginary argument. [J. Petzold, Sitzber. Heidelberger Akad. Wiss. Math.—naturw. Kl. Abhandl. 5 (1960/61). See also B. Kaufman, and H. J. Lipkin, Ann. Phys. (New York) **18**, 294 (1962).] The correction factor reduces to unity (a) for $T=0$, (b) for an infinite lattice when no (high frequency) localized mode exists. For finite temperature and a localized mode the correction is $I_0(2W_{LM}/\sinh(\hbar\omega_{LM}/2kT))$, where W_{LM} is the contribution of the localized mode to W for $T=0,\cdots$, and ω_{LM} is the localized mode frequency. In the case of Fe^{57} this Bessel function differs from unity by at most a few percent unless the temperature is large compared with the Debye temperature, which invalidates the theory anyway. W_{LM} can be obtained from Figs. 3, 5, and 7.

Each λ_μ is doubly degenerate, and the u's satisfy

$$\textstyle\sum_\alpha \mu_\alpha^{(\mu)}\mu_\alpha^{(\nu)}=\delta_{\mu\nu}. \tag{13}$$

From Eqs. (9) and (13), Eq. (8) immediately follows.

We are now in a position to calculate the determinant of Eq. (5).

$$\begin{aligned}D(\omega^2)&=\mathrm{Det}(L_{\alpha\beta}-P_{\alpha\beta})\\&=\mathrm{Det}L_{\alpha\beta}\,\mathrm{Det}(\delta_{\alpha\beta}-\textstyle\sum_\gamma g_{\alpha\gamma}P_{\gamma\beta})\\&=D_0(\omega^2)D_1(\omega^2)\end{aligned} \tag{14}$$

The first factor of $D(\omega^2)$ is exactly the determinant of the system of equations for $a=\delta\mu=\delta\gamma=0$. The second factor reduces to unity for this case, and is in the general case the determinant of a 3×3 matrix, since $P_{\gamma\beta}=0$ unless γ and β are -1, 0, or $+1$.

$D(\omega^2)$ is a polynomial of order $2N+1$ in ω^2, and has zeros at each normal mode frequency. Any additive function of the frequencies can therefore be written (see Montroll and Potts[5])

$$\sum_s f(\omega_s)=\frac{1}{2\pi i}\int_c f(\omega)d\ln D(\omega^2), \tag{15}$$

where the sum on the left is over all the normal mode frequencies, and the contour on the right is counterclockwise around that portion of the positive real axis in which the zeros of D occur. If, in particular, we choose

$$f(\omega_s)=\hbar\omega_s(n_s+\tfrac{1}{2}), \tag{16}$$

then Eq. (15) becomes the total energy of the system in a state specified by the occupation numbers n_s.

$$\langle\{n_s\}|H|\{n_s\}\rangle=\sum_s f(\omega_s). \tag{17}$$

The derivative of the total energy with respect to a is, according to Eq. (3), equal to the Debye-Waller factor, Eq. (2), for the system in state $\{n_s\}$.

$$W(\{n_s\})=\sum_s(n_s+\tfrac{1}{2})\hbar\left.\frac{\partial\omega_s}{\partial a}\right|_{a=0}. \tag{18}$$

Because each n_s occurs at most linearly in Eq. (18), the thermal average is accomplished by simply replacing n_s by its value at thermal equilibrium, and Eq. (2) becomes

$$W=\frac{\hbar}{2\pi i}\int_c[n(\omega,T)+\tfrac{1}{2}]\left.\frac{\partial\omega}{\partial a}\right|_{a=0}d\ln D(\omega^2), \tag{19}$$

where

$$n(\omega,T)=(e^{\hbar\omega/kT}-1)^{-1}. \tag{20}$$

The normal mode frequencies occur where $D(\omega^2)=0$, and we can therefore equate

$$\left.\frac{\partial\omega}{\partial a}\right|_{a=0}=-\frac{\partial D(\omega^2)}{\partial a}\Big/\left.\frac{\partial D(\omega^2)}{\partial\omega}\right|_{a=0}. \tag{21}$$

Thus

$$W=\frac{-\hbar}{2\pi i}\int_c [n(\omega,T)+\tfrac{1}{2}]\frac{\partial D(\omega^2)}{\partial a}\Big/ D(\omega^2)\Big|_{\alpha=0} d\omega. \quad (22)$$

We now turn our attention to the calculation of $D(\omega^2)$. Since $D_0(\omega^2)$ [Eq. (14)] is independent of a, it drops out of Eq. (22), and we need concern ourselves only with $D_1(\omega^2)$, which involves the Green's functions

$$g_{\alpha\beta}=\frac{1}{2N+1}\sum_{n=-N}^{N}\frac{e^{2\pi n i(\alpha-\beta)/(2N+1)}}{4\gamma\sin^2[n\pi/(2N+1)]-\mu\omega^2}. \quad (23)$$

Using a physicist's license to ignore the question of whether an integration and a limiting process may be interchanged, we proceed to take the limit of Eq. (23) as $N\to\infty$. Then

$$g_{\alpha\beta}(\omega^2)\to\frac{1}{\pi}\int_0^\pi d\varphi\frac{\cos(\alpha-\beta)\varphi}{4\gamma\sin^2(\varphi/2)-\mu\omega^2}. \quad (24)$$

and we notice a difficulty characteristic of the one-dimensional chain, namely, as $N\to\infty$, so does $g_{\alpha\beta}(0)$ and $g_{\alpha\beta}(4\gamma/\mu)$. We avoid this trouble by cutting off the contour in Eq. (22) at $\mathrm{Re}\omega=\eta=O((\pi/N)(\gamma/\mu)^{1/2})$ and at $\mathrm{Re}\omega=(4\gamma/\mu)-\eta$.

The integral in Eq. (24) can be performed,[8] yielding

$$g_{\alpha\beta}(\xi)=\frac{-i^{|\alpha-\beta|+1}[(1-\xi^2)^{1/2}+i\xi]^{|\alpha-\beta|}}{2(1-\xi^2)^{1/2}}, \quad (25)$$

where

$$\begin{aligned}\xi&=1-2x^2,\\ x&=\omega/\omega_L,\\ \omega_L&=(4\gamma/\mu)^{1/2}.\end{aligned} \quad (26)$$

We have taken $\mathrm{Im}x>0$ and the branch of the square root for which

$$|(1-\xi^2)^{1/2}-i\xi|>1. \quad (27)$$

Using Eqs. (6) and (14) one can easily evaluate $D_1(\omega^2)$. It is

$$\begin{aligned}D_1(\omega^2)&=[(g_2-g_0)\delta\gamma-1]\\ &\quad\times\{(\delta\mu\omega^2-ak^2)[g_0+\delta\gamma(g_0^2-2g_1^2+g_0g_2)]\\ &\qquad-\delta\gamma(3g_0-4g_1+g_2)-1\} \quad (28)\\ &=D_2(\omega^2)D_3(\omega^2),\end{aligned}$$

where $g_k=g_{\alpha\beta}$ for $|\alpha-\beta|=k$. The first factor $[D_2(\omega^2)]$ in Eq. (28) will drop out of Eq. (22) because its zeros are modes in which the impurity atom is stationary. The zeros of the other factor (imagining for the moment that the limit $N\to\infty$ has not yet been taken) are the remainder of the normal modes. So Eq. (22) becomes

$$W=\frac{\hbar k^2}{2\pi i}\int_c[(n(\omega,T)+\tfrac{1}{2})]\times\frac{g_0+\delta\gamma(g_0^2-2g_1^2+g_0g_2)}{D_3(\omega^2)|_{\alpha=0}}d\omega. \quad (29)$$

The contour c encircles the roots of D_3 on the positive reals axis. These roots become dense in the range $0<\omega^2<\omega_L^2$ as $N\to\infty$, and one (the localized mode) may break off and have a higher frequency.[5] We therefore study the behavior of $D_3(\omega^2)$ for $N\to\infty$. For the sake of simplicity we consider the case of an isotopic impurity with $\delta\gamma=0$. Then the fraction in the integral [Eq. (29)] becomes

$$\frac{\partial D(\omega^2)}{\partial a}\Big/D(\omega^2)\Big|_{a=0}=\frac{k^2}{2\gamma}\left[\frac{\delta\mu}{\mu}(1-\xi)-i(1-\xi^2)^{1/2}\right]^{-1}, \quad (30)$$

which has a simple pole at

$$x_{LM}^2=[1-(\delta\mu/\mu)^2]^{-1} \quad (31)$$

if $\delta\mu<0$; otherwise it has no positive poles. To make the square root single valued, its two branch points at $\xi=\pm1$ must be connected by a cut, which we put on the real axis. Then the contour c can be contracted, and the integral [Eq. (29)] splits into two parts—one contribution from the cut and one from the residue at the pole of Eq. (31) if $\delta\mu<0$. Then if we further simplify Eq. (29) by letting $T=0$,

$$W=\frac{R}{\hbar\omega_L}\left[\frac{1}{\pi}\int_0^1\frac{(1-x^2)^{1/2}}{1-x^2(1-Q^2)}\frac{dx}{x}+\left(\frac{Q^2}{1-Q^2}\right)^{1/2}\right], \quad (32)$$

with $Q=\delta\mu/\mu$, $R=\hbar^2k^2/2\mu$, and where the last term is the contribution of the localized mode which is omitted if $Q>0$. The integral is elementary and yields[9]

$$\begin{aligned}W&=\frac{R}{\hbar\omega_L}\left[\frac{1}{2\pi}\ln\frac{2}{\epsilon}-\frac{1}{\pi}\left(\frac{Q^2}{1-Q^2}\right)^{1/2}\right.\\ &\quad\left.\times\tan^{-1}\left(\frac{1-Q^2}{Q^2}\right)^{1/2}+\left(\frac{Q^2}{1-Q^2}\right)^{1/2}\right] \quad -1<Q<0\\ &=\frac{R}{\hbar\omega_L}\left[\frac{1}{2\pi}\ln\frac{2}{\epsilon}-\frac{1}{\pi}\left(\frac{Q^2}{1-Q^2}\right)^{1/2}\tan^{-1}\left(\frac{1-Q^2}{Q^2}\right)^{1/2}\right]\\ &\qquad 0<Q<1\\ &=\frac{R}{\hbar\omega_L}\left[\frac{1}{2\pi}\ln\frac{2}{\epsilon}-\frac{1}{\pi}\left(\frac{Q^2}{Q^2-1}\right)^{1/2}\tanh^{-1}\left(\frac{Q^2-1}{Q^2}\right)^{1/2}\right]\\ &\qquad Q>1, \quad (33)\end{aligned}$$

where ϵ is a cutoff introduced to make the integral in Eq. (32) converge at its lower limit. The mean square

[8] G. N. Watson, *Theory of Bessel Functions*, (Cambridge University Press, New York, 1944), 2nd ed., p. 386.

[9] *Proceedings of the Second International Conference on the Mössbauer Effect* (John Wiley & Sons, Inc., New York, 1962), p. 30.

displacement of a particle in an infinite chain is infinite, and ϵ effectively removes the very long wavelengths. This is a difficulty which does not occur in 2 or 3 dimensions.

The contribution of the localized mode is the third term in the first of Eqs. (33). As $Q\rightarrow -1$ ($\mu'\rightarrow 0$) it increases as $(\mu')^{-1/2}$, which is what one should expect in this limit since then the impurity moves in what amounts to a static potential. It should also be noticed that the value of W *and its slope* are continuous across $Q=0$. This happens because of the appearance of the localized mode at $Q=0$. It will be found to hold true in three dimensions, too, although there the localized mode will not appear until Q becomes appreciably negative.

Other quantities which we calculate in the one-dimensional model to illustrate the methods to be used in three dimensions are $\partial\langle H\rangle/\partial\mu'$ from which one could obtain the Josephson shift[3] if we were not limiting our one-dimensional calculations to $T=0$, and the spectrum shape to be expected in a rotor experiment.[4] Since we have in fact, already calculated the latter, we consider it first.

By comparison of Eq. (32) with known expressions for the spectrum[10] one can easily see that the shape for $T=0$ is just twice the integrand.

$$w_1(E)dE=e^{-2W}\frac{2R}{\hbar\omega_L}\left[\frac{1}{\pi}\frac{(1-x^2)^{1/2}}{1-x^2(1-Q^2)}\frac{dx}{x}+\delta(x-x_{LM})\left(\frac{Q^2}{1-Q^2}\right)^{1/2}dx\right]. \quad (34)$$

The first term contributes only for $0<x<1$; the second for $-1<Q<0$. As one might have foreseen, w_1 is singular at $x=0$ because the density of states for the linear chain does not vanish there. The "spectrum" implied by Eq. (34) is proportional to $(1-x^2)^{-1/2}$ for a perfect lattice ($Q=0$), and is equal to the phonon spectrum, but for $Q\neq 0$ it loses its singularity at $x=1$ and quickly becomes badly distorted. For $Q\gg 1$, the continuum becomes compressed into a peak at the origin of half-width Q^{-1}; something similar will happen in three dimensions, except the peak will occur at a positive frequency.[6]

The velocity shift is calculated by a method very similar to that used to find W. We define [compare Eq. (18)]

$$V(\{n_s\})=\sum_s(n_s+\tfrac{1}{2})\hbar\frac{\partial\omega_s}{\partial\mu'}, \quad (35)$$

and in several steps obtain the analog of Eq. (22),

$$V=-\frac{\hbar}{2\pi i}\int_c\left[n\left(\omega,T\right)+\frac{1}{2}\right]\frac{\partial D(\omega^2)}{\partial\mu'}\Big/D(\omega^2)\Big|_{a=0}d\omega, \quad (36)$$

which leads, for $T=\delta\gamma=0$, to

$$V=-\frac{\hbar\omega_L}{2\mu}\left[\frac{1}{\pi}\int_0^1\frac{(1-x^2)^{1/2}xdx}{1-x^2(1-Q^2)}+\frac{|Q|}{(1-Q^2)^{3/2}}\right]. \quad (37)$$

This can be expressed, like Eq. (33), in terms of inverse hyperbolic and trigonometric functions.

III. THE THREE-DIMENSIONAL CASE

The formal steps are nearly identical in the three- and one-dimensional cases, but in three dimensions not even the simplest cases can be carried through analytically. In this section we derive expressions for the various observable quantities,[11] and in the next describe their numerical evaluation.

The Hamiltonian we shall use for the imperfect crystal is

$$\begin{aligned}H_0=&\tfrac{1}{2}\sum_{ijk}\mu\dot{x}_{ijk}^2+\tfrac{1}{2}\sum_{ijk}[\gamma_1(x_{i+1jk}-x_{ijk})^2+\gamma_1(x_{i-1jk}\\&-x_{ijk})^2+\gamma_2(x_{ij+1k}-x_{ijk})^2+\gamma_2(x_{ij-1k}-x_{ijk})^2\\&+\gamma_3(x_{ijk+1}-x_{ijk})^2+\gamma_3(x_{ijk-1}-x_{ijk})^2]+\tfrac{1}{2}\delta\mu\dot{x}_{000}^2\\&+\tfrac{1}{2}\delta\gamma_1[(x_{100}-x_{000})^2+(x_{-100}-x_{000})^2]\\&+\tfrac{1}{2}\delta\gamma_2[(x_{010}-x_{000})^2+(x_{0-10}-x_{000})^2]\\&+\tfrac{1}{2}\delta\gamma_3[(x_{001}-x_{000})^2+(x_{00-1}-x_{000})^2]\\&+\text{similar terms in } y \text{ and } z, \quad (1')\end{aligned}$$

and we immediately make the restriction that $\gamma_1=\gamma_2=\gamma_3=\gamma$ and $\delta\gamma_1=\delta\gamma_2=\delta\gamma_3=\delta\gamma$ in order to reduce the number of variable parameters and simplify the numerical work. Equation (1′) then describes a simple cubic crystal with nearest-neighbor harmonic interactions of the type used by Montroll and Potts,[5] with an impurity at the (0,0,0) lattice site with mass $\mu'=\mu+\delta\mu$ and force constant (between it and its six nearest neighbors) $\gamma'=\gamma+\delta\gamma$.

It is easy to show[12] that Mössbauer emission from our lattice is isotropic; we therefore may take $\mathbf{k}$ along the x axis, without loss of generality. Then the motions along the three Cartesian axes are separable, and only the normal modes involving displacements in the x direction need concern us.

$$\begin{aligned}H&=H_0+H_1,\\H_1&=\tfrac{1}{2}a(kx_{000})^2.\end{aligned} \quad (3')$$

The classical equations of motion are

$$\mu\ddot{x}_{ijk}-\gamma(x_{i+1jk}+x_{i-1jk}+x_{ij+1k}+x_{ij-1k}+x_{ijk+1}+x_{ijk-1}-6x_{ijk})=\sum_{\alpha\beta\gamma}P_{ijk,\alpha\beta\gamma}x_{\alpha\beta\gamma}, \quad (4')$$

[10] See, for example, (reference 7, Sec. 6). What we call the spectrum is really the 1-phonon part of the spectrum, which is the major contribution for $R/\hbar\omega_L\ll 1$.

[11] Three dimensional analogs of the equations appearing in Sec. II are denoted by primes.

[12] The cross products in W, like $\langle xy\rangle_T$, vanish, and the diagonal terms are all equal. $\langle x^2\rangle_T=\langle y^2\rangle_T=\langle z^2\rangle_T$.

or

$$\sum_{\alpha\beta\gamma} L_{ijk,\alpha\beta\gamma}x_{\alpha\beta\gamma}=\sum_{\alpha\beta\gamma} P_{ijk,\alpha\beta\gamma}x_{\alpha\beta\gamma}, \tag{5'}$$

where L is an $N\times N$ matrix, but P is only 7×7. Letting $\ddot{x}_{ijk}=-\omega^2 x_{ijk}$, it is

$$P=\begin{Bmatrix} -\delta\gamma & 0 & 0 & \delta\gamma & 0 & 0 & 0 \\ 0 & -\delta\gamma & 0 & \delta\gamma & 0 & 0 & 0 \\ 0 & 0 & -\delta\gamma & \delta\gamma & 0 & 0 & 0 \\ \delta\gamma & \delta\gamma & \delta\gamma & P_0 & \delta\gamma & \delta\gamma & \delta\gamma \\ 0 & 0 & 0 & \delta\gamma & -\delta\gamma & 0 & 0 \\ 0 & 0 & 0 & \delta\gamma & 0 & -\delta\gamma & 0 \\ 0 & 0 & 0 & \delta\gamma & 0 & 0 & -\delta\gamma \end{Bmatrix}, \tag{6'}$$

$$100 \quad 010 \quad 001 \quad 000 \quad 00\text{–}1 \quad 0\text{–}10 \quad -100$$

where

$$P_0=\delta\mu\omega^2-ak^2-6\delta\gamma, \tag{38}$$

and the numbers written below the columns are also the order of the rows. With trivial generalizations, the definition of Green's functions and the formal factorization of the secular determinant are exactly as before. We find

$$\lambda_\mu=4\gamma\sum_{\alpha=1}^{3}\sin^2(\tfrac{1}{2}\varphi_\alpha{}^\mu)-\mu\omega^2, \tag{11'}$$

and

$$g_{\mathbf{k},\boldsymbol{\alpha}}=\frac{1}{N^3}\sum_{\mu}\frac{\exp[2\pi i\boldsymbol{\varphi}^\mu\cdot(\mathbf{k}-\boldsymbol{\alpha})/N]}{4\gamma\sum_{\beta=1}^{3}\sin^2(\varphi_\beta{}^\mu/2)-\mu\omega^2}. \tag{23'}$$

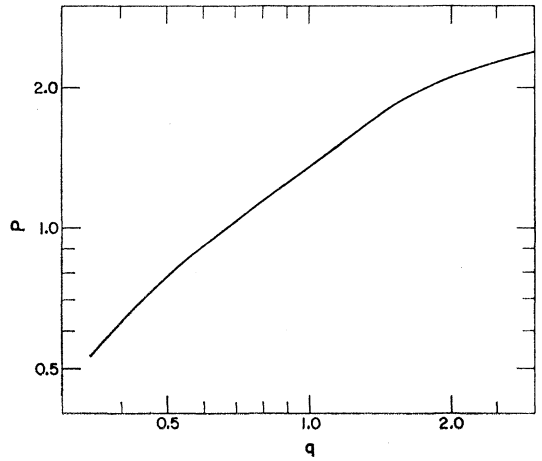

FIG. 2. Locus in the $p-q$ plane at which the localized mode appears. The localized mode exists above the curve, disappears below it. Contrary to the situation for a finite lattice, where the curve would pass through (1,1), the appearance of the localized mode is delayed for an infinite lattice until, roughly $q<0.67\ p^{4/3}$. [G. F. Nardelli and N. Tettamanzi, Phys. Rev. **126**, 1283 (1962), have found that the appearance of the localized mode for an isotopic ($p=1$) impurity is delayed for an fcc lattice until $q=0.78$.] The frequency of the localized mode increases above the line. At a distance of about log 2 from the line on the lower side, an "approximate localized mode"[6] begins to appear at low frequency. Its frequency decreases and it becomes higher and sharper with increasing distance below the curve.

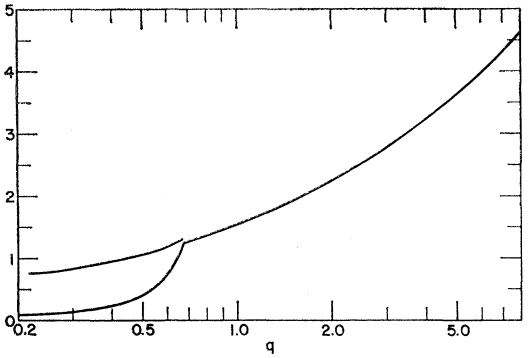

(a)

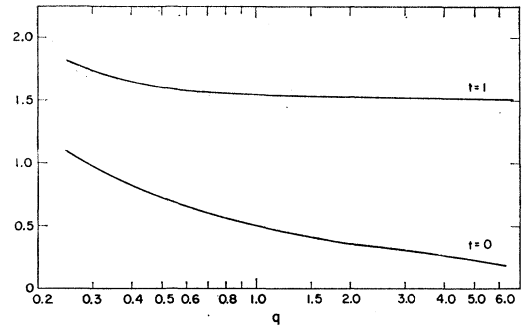

(b)

FIG. 3. (a) This curve shows $2W_D$ for $t=0$, $p=1$, as a function of q. The localized mode appears below $q=0.67$, where the lower curve is the contribution of the continuous spectrum to $2W_D$. The localized mode accounts for most of the mean square displacement. The ordinate, when multiplied by $-R'/\hbar\omega_L$, is equal to the logarithm of the recoilless fraction. The Debye temperature for this model, as determined by fitting a parbola to the bottom of the phonon spectrum, is given by $k\theta_D=1.1\hbar\omega_L$. (b) V_D for $p=1$, $t=0$, and $t=1$. To get the fractional shift for Fe^{57} from these data one should multiply the ordinate by 5.5×10^{-13} $(\theta_D/330)$; the velocity shift is 0.166 $(\theta_D/330)$ mm/sec. Notice also that in this curve, as well as in Figs. 5(b) and 7(b), the high temperature limit, which is $\frac{3}{2}t$ for the quantity plotted here, is attained for $t=1$ when there is no localized mode.

Since $g_{\mathbf{k},\boldsymbol{\alpha}}=g(|\mathbf{k}-\boldsymbol{\alpha}|)$, we need only four of these functions, namely,

$$\begin{aligned} g_{000,000}&=g_0=\frac{i}{2\gamma}\int_0^\infty d\alpha\, e^{-i\alpha\xi}J_0{}^3(\alpha) \\ g_{100,000}&=g_1=-\frac{1}{2\gamma}\int_0^\infty d\alpha\, e^{-i\alpha\xi}J_1(\alpha)J_0{}^2(\alpha) \\ g_{110,000}&=g_{11}=-\frac{i}{2\gamma}\int_0^\infty d\alpha\, e^{-i\alpha\xi}J_1{}^2(\alpha)J_0(\alpha) \\ g_{200,000}&=g_2=-\frac{i}{2\gamma}\int_0^\infty d\alpha\, e^{-i\alpha\xi}J_2(\alpha)J_0{}^2(\alpha). \end{aligned} \tag{25'}$$

These equations are derived by taking $N\to\infty$ and using an integral representation for the Bessel functions.

They are written here for $\mathrm{Im}x>0$, where

$$\xi=3(1-2x^2),$$
$$x=\omega/\omega_L, \qquad (26')$$
$$\omega_L=(12\gamma/\mu)^{1/2}.$$

The integrals in Eqs. (25′) cannot be expressed in closed form, except some of them in terms of the others. Their evaluation constitutes most of the numerical work required for this problem.

We can now write down the secular determinant

$$D_1(\omega^2)=\mathrm{Det}(\delta_{ijk,\alpha\ \gamma}-\sum_{lmn} g_{ijk,lmn}P_{lmn,\alpha\beta\gamma}), \qquad (14')$$

which has rank N, but since P is 7×7 the rank fortunately is reducible to 7. On performing the matrix multiplication and evaluating the determinant, one finds

$$D_1(\omega^2)=D_2(\omega^2)D_3(\omega^2)$$
$$D_2(\omega^2)=[1-(g_2-g_0)\delta\gamma]^3[1-(2g_{11}-g_0-g_2)\delta\gamma]^2$$
$$D_3(\omega^2)=[1-g_0(\delta\mu\omega^2-ak^2)][1-(6g_1-4g_{11}-g_0-g_2)\delta\gamma]$$
$$+6[1-g_1(\delta\mu\omega^2-ak^2)](g_0-g_1)\delta\gamma. \qquad (28')$$

Here, as in one dimension, D_2 is irrevelant to any calculation of the motion of the impurity atom, since it is independent of $\delta\mu$ and a. Therefore, in the integrals for W [Eq. (22)] and V [Eq. (36)] D can be replaced by D_3. $\partial D_3/\partial a$ and $\partial D_3/\partial\mu'$ may be written down by inspection of Eq. (28′). Then

$$W=\frac{i\hbar}{\pi}\int_0^{\omega_L}d\omega\left[n(\omega,T)+\frac{1}{2}\right]\mathrm{Im}\frac{\partial D_3(\omega^2)/\partial a}{D_3(\omega^2)}\bigg|_{a=0}$$
$$-\hbar\left[n(\omega,T)+\frac{1}{2}\right]\frac{\partial D_3(\omega^2)/\partial a}{\partial D_3(\omega^2)/\partial\omega}\bigg|_{\omega=\omega_{LM},a=0}, \qquad (32')$$

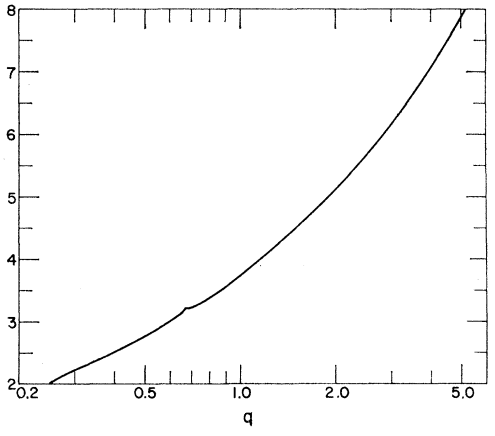

FIG. 4. These are the factors by which the curve of Fig. 3(a) should be multiplied to get its value for $t=1$. The rapid rise for large q reflects the fact that the spectrum is bunching up at small values of x; the decrease as q drops for $q>0.67$ indicates bunching up at high x; the continued decrease is due to the fact that more and more of the amplitude is going into the localized mode, whose frequency increases.

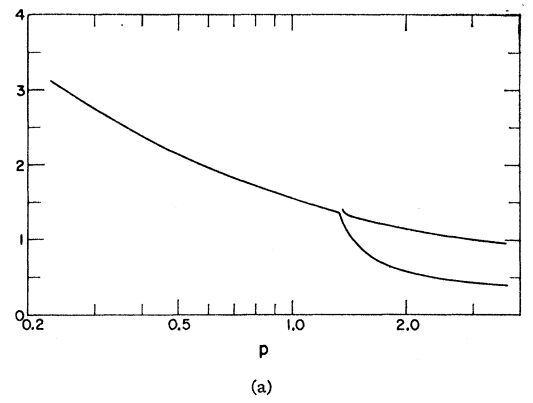

(a)

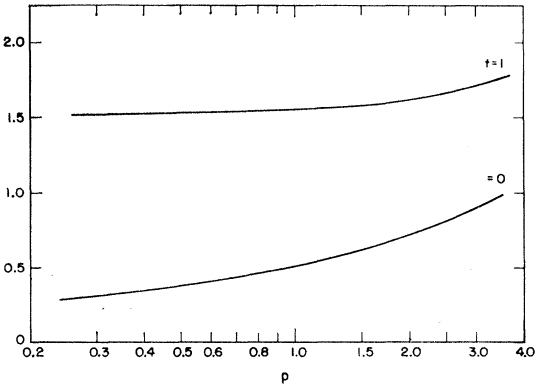

(b)

FIG. 5. (a) $2W_D$ for $t=0$, $q=1$. The localized mode appears for $p>1.35$. See caption of Fig. 3(a). (b) V_D for $q=1$, $t=0$, and $t=1$. See caption of Fig. 3(b).

where ω_{LM} is the localized mode frequency which is found numerically by locating the zero of D_3 for $\omega>\omega_L$. D_3 and all the g's are real in this range.

Similarly we find

$$V=\frac{-3i\hbar}{\pi}\int_0^{\omega_L}d\omega\left[n(\omega,T)+\frac{1}{2}\right]\mathrm{Im}\frac{\partial D_3(\omega^2)/\partial\mu'}{D_3(\omega^2)}\bigg|_{a=0}$$
$$+3\hbar\left[n(\omega,T)+\frac{1}{2}\right]\frac{\partial D_3(\omega^2)/\partial\mu'}{\partial D_3(\omega^2)/\partial\omega}\bigg|_{\omega=\omega_{LM}a=0}, \qquad (37')$$

which differs only slightly from Eq. (32′) because $\omega^2\partial D_3/\partial a=-k^2\partial D_3/\partial\mu'$. The factor 3 occurs in V but but not in W, because the latter is proportional to the mean square displacement in only one direction.

The one-phonon spectrum can also be obtained by inspection of Eq. (32′), viz.,

$$w_1(E)dE=e^{-2W}\hbar\left[\frac{i}{\pi}\mathrm{Im}\frac{\partial D_3/\partial a}{D_3}\right.$$
$$\left.-\frac{\partial D_3/\partial a}{\partial D_3/\partial\omega}\delta(\omega-\omega_{LM})\right]d\omega, \qquad (34')$$

which is valid for $T=0$. For finite temperatures, Eq. (34′) should be multiplied by $[n(\omega,T)+1]$ or $n(\omega,T)$ to get the absorption or emission spectra, respectively.

IV. NUMERICAL CALCULATIONS AND RESULTS

An IBM 7090 was used for the computing. The program first evaluates the real and imaginary parts of certain linear combinations of the Green's functions as given by Eq. (25′) using Simpson's rule for the numerical integrations and cutting off the upper limit of the integral when the contributions become negligible. These functions are evaluated at from 50 to 200 values of x^2. Then D_3 and its derivatives with respect to a and μ' are calculated at the same points, and the integrals for V and W are calculated, again by Simpson's rule. A search is made for the zero of D_3 for $x^2>1$; if such exists, $\partial D_3/\partial\omega$ is evaluated at that point and the localized mode contributions are added to V and W. The amount of machine time required is quite small; 15 or 20 min would suffice to repeat all the calculations done for this paper.

The quantities

$$W_D=(\hbar\omega_L/R')W,\qquad V_D=-(\mu'/\hbar\omega_L)V, \tag{39}$$

where

$$R'=\hbar^2k^2/2\mu', \tag{40}$$

are dependent only on three parameters, namely,

$$q=\mu'/\mu,\qquad p=\gamma'/\gamma,\qquad t=kT/\hbar\omega_L. \tag{41}$$

The range of values of these parameters for which calculations have been done is

$$0.3<q<5,\qquad 0.3<p<3,\qquad t=0,\ 1. \tag{42}$$

For smaller impurity masses the localized mode frequency becomes too large for the calculation of the g's to be accurate with the interval size used. For larger impurity masses the spectrum acquires a high, narrow peak for small x^2, which makes the calculation meaningless when its width becomes comparable to the interval used in the numerical integration. For small p the same thing happens as for large q; for large p the same as for small q. These limitations are only practical ones. The range could easily be extended if it were interesting to do so. Only two values of the temperature have been used.

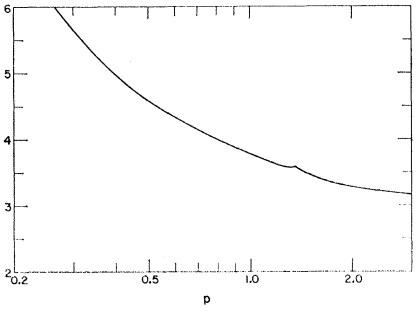

FIG. 6. Temperature factor appropriate to Fig. 5(a). See caption of Fig. 4.

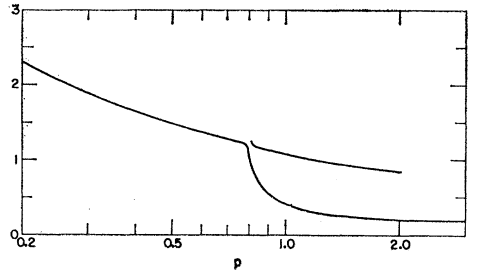

(a)

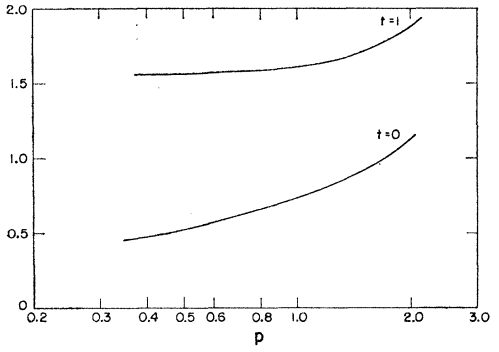

(b)

FIG. 7. (a) $2W_D$ for $t=0$, $q=0.5$. The localized mode appears for $p>0.80$. See caption of Fig. 3(a). (b) V_D for $q=0.5$, $t=0$, and $t=1$. See caption of Fig. 3(b).

Figure 2 shows the region of p-q space in which the high frequency localized mode exists. The appearance of this mode is reflected in the branching of Fig. 3(a) below $q=0.67$ where the contributions of the localized mode and of the phonons to the mean square displacement are plotted separately for the case of an isotopic impurity. Figure 3(b) shows the behavior of the mean square velocity of the isotopic impurity. Figure 4 gives the ratio of the mean square displacement for $t=1$ to that for $t=0$. The rapid rise for increasing q reflects a decrease in the dominant frequencies of oscillation for the heavy impurity. Figures 5 and 6 exhibit the corresponding results for an impurity with the host's mass, but variable coupling constant, and Figs. 7 and 8 show the same quantities for an impurity of half the host's mass as a function of force parameter.

In Figs. 9 and 10 we show the shapes of the one-phonon absorption cross sections for $T=0$ as functions of the square of the phonon energy. These graphs clearly

illustrate that the host lattice phonon spectrum is well disguised unless p and q are both near unity.

An unexpected result of the calculation is that over the limited range of p, $q=1.0\pm0.5$, the Einstein model seems to explain the variation of W at $T=0$. That is, to within about 3%,

$$2W=1.55R'/\hbar\omega_L', \tag{43}$$

where $\omega_L'=(12\gamma'/\mu')^{1/2}$.

Equation (43) contradicts an argument made by Shapiro[13] to the effect that the mean square displacement should be independent of the impurity mass. It seems, in fact, to be independent of the *host* mass, and also of the host lattice stiffness. Where Eq. (43) has a factor of 1.55, the Einstein model would predict a factor of unity, a difference which may be interpreted as due to the difference between an average vibrational frequency and ω_L'. The mean square velocity also fits into this picture; V_D for $t=0$ [Figs. 3(b), 5(b), and 7(b)] is proportional to $(p/q)^{1/2}$ over a fairly wide range of values for p and q.

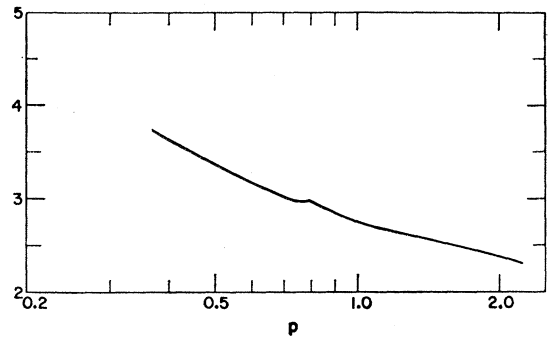

FIG. 8. Temperature factor appropriate to Fig. 7(a). See caption of Fig. 4.

The dependence of the localized mode frequency on p and q is shown in Figs. 11 and 12. After some curvature near the point of appearance, each of these curves is very nearly a straight line. This is again consistent with the Einstein model, which would, however, predict that the lines should pass through the point $p,q=1,1$. An asymptotic solution (for $x^2\gg1$) of the secular equation yields the result that the localized mode frequency should be

$$x_{LM}^2=\text{const}+\tfrac{1}{2}p(q^{-1}+1/6), \tag{44}$$

which, in fact, fits the linear parts of Figs. 11 and 12 quite well if the constant is put equal to 0.07.

The localized mode amplitude can be seen from Figs. 3, 5, and 7 to rise rapidly after the point of appearance, then stay fairly constant. The maximum amplitude attained over the range studied is between 0.6 and $0.8R'/\hbar\omega_L$ of the Mössbauer amplitude, indicating that it should be easily detectable if one could obtain the proper energy in a Mössbauer beam.[14]

[13] F. L. Shapiro, Uspekhi Fiz. Nauk. **72**, 685 (1960) [translation: Soviet Phys.—Uspekhi **3**, 881 (1961)]. Shapiro's argument is outlined by Fraunfelder (reference 1, p. 84).

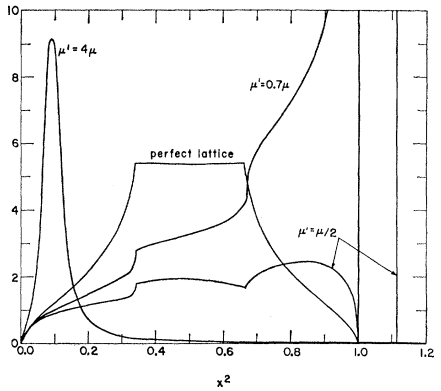

FIG. 9. The spectra as given by Eq. (34′) for several values of q for $p=1$. The perfect lattice spectrum is familiar;[5] the $q=4$ case illustrates the low frequency "approximate localized mode" which becomes much higher, narrower, and lower in frequency for larger q values. The $q=0.7$ case illustrates the bunching at high frequencies just before the localized mode is pushed out, and the $q=0.5$ case shows the situation after the localized mode has become fairly well developed. The dimensionless ordinate here should be multiplied by $k^2e^{-2W}/12\gamma\pi$ to get $w_1(E)$.

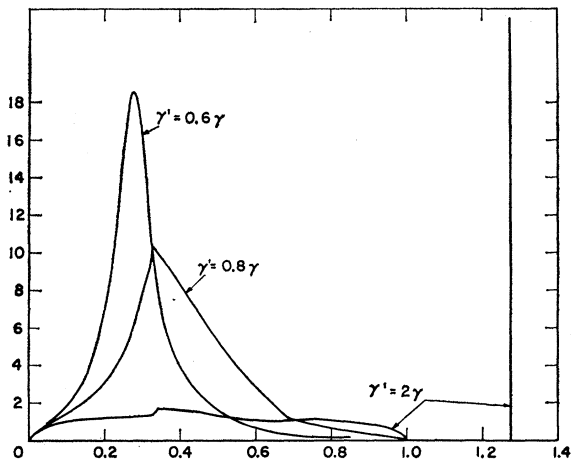

FIG. 10. Same as Fig. 9, except here $q=1$ and p is varied. The spectra for this case have many of the same qualitative features as those of Fig. 9, including the appearance of both kinds of localized modes. The low-frequency "localized mode" appears here; for any reasonable values of γ' its frequency is higher than that of a heavy impurity. It can, however, become very sharp and high for unrealistic values of γ'; for example, if $\gamma'=0.1\gamma$ the peak occurs at $x^2=0.05$ with a width of 0.01 and a height of several hundred on the scale of this graph.

[14] B. Mozer, K. Otnes, and V. Myers [Phys. Rev. Letters **8**, 278 (1962)] have observed the localized mode by scattering neutrons from a nickel-palladium alloy. This is perhaps easier than using γ rays, because of the high Doppler velocities required in the latter case. The high velocities could, however, possibly be avoided by having the localized mode preferentially excited in the emitter; then an appreciable fraction of the gammas would have the right energy to be absorbed with excitation of the localized mode in the absorber. If the localized mode lifetime is comparable

The low frequency peak[6] for high masses or low coupling constants should be easier to find by Mössbauer techniques because of the lower Doppler velocities required. For no force constant difference, its position is approximately $x^2=0.3\mu/\delta\mu$; its height increases and its width decreases with increasing $\delta\mu$.

V. SUMMARY AND DISCUSSION

We have considered the dynamics of a simple cubic crystal model with harmonic forces, and allowed the mass and coupling of a single atom in this lattice to differ from the rest. In the limit of an infinite host lattice the significant results are: (a) the continuity of the mean square displacement of the impurity atom across the point of appearance of the localized mode, and its independence of the properties of the host lattice; (b) additionally, the mean square velocity is independent of the properties of the host. (c) The spectrum is strongly dependent on the impurity parameters. It is simply related to the host lattice phonon spectrum only when mass and coupling constant ratios (q and p) are close to unity. (d) The square of the localized mode frequency is a linear function of p and of $1/q$, and its amplitude is comparable to the Mössbauer peak. (e) For high q or low p a low frequency localized mode appears which can dominate the spectrum.

The known experimental data with which results (a) and (b) might be compared are very meager. Since our results are quite close to the results of the Debye model for a perfect lattice, we need measurements, say, of the recoilless fraction f for active atoms in a host which differs either in mass or coupling or both. There are only two pieces of data of this type that we know of, namely, Fe in Be,[15] and Fe in In.[16] The former can be accounted for nicely with our theory, the latter not at all because of its low value of f and its virtual independence of temperature. It would require an *ad hoc* assumption of a temperature-dependent p to reduce the temperature dependence of f. Or possibly this is a manifestation of gross anharmonicity in the binding.[16] No data bear on results (c) or (e); they are, however, amenable to study with neutrons as well as with the Mössbauer effect. Result (d) has some relevance to the nickel-palladium experiment[14].

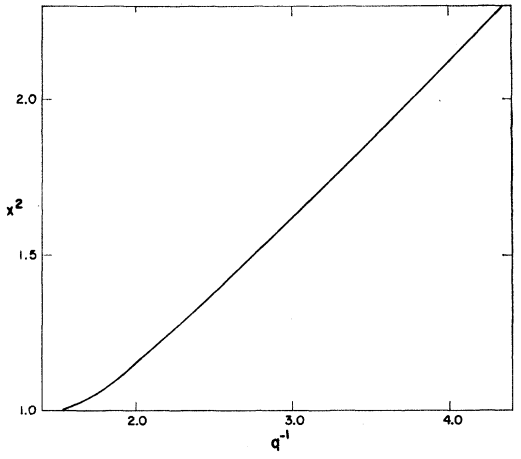

FIG. 11. Square of localized mode frequency in units of ω_L for $p=1$ as a function of q^{-1}. See discussion in text.

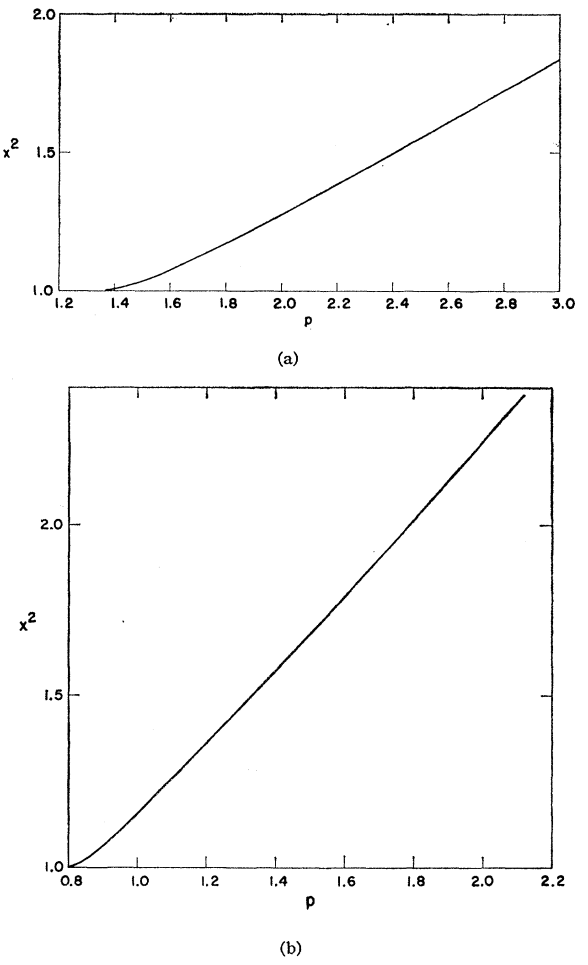

FIG. 12. Square of localized mode frequency in units of ω_L for (a) $q=1$, (b) $q=\frac{1}{2}$, as a function of p. See discussion in text.

to or longer than the 14-keV level lifetime in Fe^{57}, this would happen automatically because it would be strongly excited by the recoil caused by the 123-keV gamma emitted when the 14-keV state is formed. Filtering the resultant beam through iron would leave nearly pure "localized mode" gamma rays.

[15] J. Heberle, P. N. Parks, and J. P. Schiffer. A preliminary account of this work appears in Argonne National Laboratory Report ANL-6455 (unpublished). *Note added in proof.* The Argonne group (private communication from J. P. Schiffer) has recently measured relative f values and mean square velocities for Fe^{57} in Be, Cu, W, and Pt. Their results are consistent with our calculations for $\delta\gamma=0$. The measurements of f for Au^{197} by Shirley *et al.* [D. A. Shirley, M. Kaplan, and P. Axel, Phys. Rev. **123**, 816 (1961)] can also be explained, but not without a force constant adjustment.

[16] W. A. Steyert and P. P. Craig, Phys. Letters **2**, 165 (1962).